Journal of Autoimmunity 100 (2019) 27–39

Contents lists available at ScienceDirect

Journal of Autoimmunity

journal homepage: www.elsevier.com/locate/jautimm

Impaired Tip60-mediated Foxp3 acetylation attenuates regulatory T cell development in rheumatoid arthritis

Qiao Su[a,1], Jun Jing[b,1], Wuguo Li[a], Jianda Ma[b], Xueling Zhang[a], Zongren Wang[a,c], Zhongyang Zhou[a], Lie Dai[b,**], Lan Shao[a,*]

[a] The Center for Translational Medicine, The First Affiliated Hospital, Sun Yat-Sen University, Guangzhou, 510080, PR China
[b] Department of Rheumatology, Sun Yat-Sen Memorial Hospital, Sun Yat-Sen University, Guangzhou, 510120, PR China
[c] Department of Urology, First Affiliated Hospital, Sun Yat-Sen University, Guangzhou, 510080, PR China

ARTICLE INFO

Keywords:
Tip60
Foxp3
Acetylation
T cell differentiation
Rheumatoid arthritis

ABSTRACT

In rheumatoid arthritis (RA), imbalanced T cells subsets play a critical role in sustaining chronic inflammatory responses in the synovium. Naïve T cells in RA patients undergo maldifferentiation, including an increase in the effector Th1/Th17 lineage and a reduction in regulatory T (Treg) cells. Upon stimulation, naïve $CD4^+CD45RO^-$ T cells from RA patients exhibited insufficient expression of Foxp3, which induced a deficiency in Tregs production and an imbalance of Treg/Th17 differentiation. Further mechanistic study indicated that RA T cells failed to produce sufficient levels of the histone acetyltransferase Tip60, leading to reduced acetylation of Foxp3; this, in turn, decreased Foxp3 expression, impaired Treg commitment, and promoted Th17 production. Moreover, in human synovium chimeric mice, suppression of Tip60 activity in healthy T cells promoted tissue infiltration and arthritogenesis, while reconstitution of Tip60 in RA T cells suppressed synovitis and effector T cell infiltration. Our findings link T cell maldifferentiation and tissue infiltration with Tip60-mediated Foxp3 acetylation and identify Tip60 as a potential therapeutic target for suppression of tissue inflammation and autoimmunogenesis in RA.

1. Introduction

Rheumatoid arthritis (RA) is a chronic autoimmune disease that is characterized by synovial inflammation and cartilage damage [1]. T cells are a critical regulator in the pathogenesis of RA as they accumulate in the lesions of joints, resulting in tissue-destruction and sustaining chronic inflammation. Memory/effector $CD4^+$ T cells help the formation of ectopic germinal centers in synovial tissue. However, T cell abnormalities in RA involve not only end-differentiated T lymphocytes that drive chronic inflammation but also the pool of unprimed naïve T cells [2–4]. The phenomena of malfunctions of naïve T cells in RA include telomere shortening, DNA damage accumulation, metabolic disorders [5–9], and an imbalanced pattern of T cell lineage differentiation that is skewed toward Th17 helper T cells rather than regulatory T (Treg) cells [10].

The imbalanced state between Th17/Treg cells and pro-/anti-inflammatory cytokines is critical for the development and progression of RA, which is in turn strongly associated with the onset of autoimmunity, chronic inflammation, and thus joint damage in RA [11]. Th17 cells lead to arthritogenic symptoms through the production of proinflammatory cytokines production, such as IL-17, TNF-α and IL-6 [11,12], whereas Tregs maintain self-tolerance by suppressing Th cells proliferation and activity through directly contact and by secretion of anti-inflammatory cytokines, such as IL-10 and TGF-β [11]. The key transcription factor that dominates Treg lineage commitment is the forkhead transcription factor Foxp3, which is also essential for maintaining the suppressive activity of mature peripheral Tregs [13,14]. Several studies have suggested that decreased Foxp3 expression leads to

Abbreviations: RA, Rheumatoid arthritis; **Treg**, Regulatory T cell; **MYST**, Mof–Ybf2–Sas2–Tip60; **TCR**, T cell receptor; **PBMCs**, Peripheral blood mononuclear cells; **SLE**, Systemic erythematosus lupus; **ACR**, American college of rheumatology; **SDS-PAGE**, Sodium dodecyl sulfate–polyacrylamide gel electrophoresis; **RIPA**, Radioimmunoprecipitation; **DAS-28**, Disease activity score-28; **MFI**, Mean fluorescence intensity; **TRB**, T cell receptor beta locus; **RANKL**, Receptor activator of nuclear factor κappa B ligand; **ESR**, Erythrocyte sedimentation rate; **DMARDs**, Disease-modifying antirheumatic drugs

* Corresponding author.
** Corresponding author.
E-mail addresses: dailie@mail.sysu.edu.cn (L. Dai), shaolan@mail.sysu.edu.cn (L. Shao).
[1] These authors contributed equally to this work.

https://doi.org/10.1016/j.jaut.2019.02.007
Received 18 July 2018; Received in revised form 2 January 2019; Accepted 10 February 2019
Available online 04 April 2019

the conversion of Tregs to Th17 effector cells [15–17]. Since an increase in the Th17 cell subset and a decrease in Tregs drives the development of autoimmune arthritis in RA patients, exploiting the molecular mechanism of Foxp3 regulation is important for understanding RA evolution.

The HIV Tat-interactive protein Tip60 is a histone acetyltransferase which belongs to the MOF–YBF2–SAS2–Tip60 (MYST) family. Emerged studies indicate that Tip60 is an important transcriptional regulator, namely, it can interact with many families of transcription factors and to exert acetyltransferase activity for multiple genes involved in the diverse cellular responses [18–20], including DNA damage repair, apoptosis, transcriptional regulation and allergies [21–26]. Tip60 enhances both the protein stability and transcriptional activity of Foxp3 by increasing the acetylation level of Foxp3 protein. Mechanism studies demonstrated that acetylation of Foxp3 protein results in increased protein levels through the prevention of Foxp3 polyubiquitination and protein degradation [27–29]. Except for regulating Treg cell differentiation, it was also demonstrated that Tip60 plays a pivotal role in regulating the reciprocally interconnected differentiation of Tregs and Th17 cells [30,31]. The interaction between Tip60 and Foxp3 suppresses the Th17-defining transcription factor RORγt. Therefore, insufficiency of the Tip60-Foxp3 complex releases the transcriptional activity of RORγt and thus expands Th17 cell differentiation. Considering the importance of the Treg/Th17 differentiation program imbalance in RA, a question was raised concerning whether Tip60-mediated Foxp3 expression contributes to this imbalance in RA disease.

Here, we reported that naïve $CD4^+$ T cells in RA patients fail to upregulate the expression of Tip60 protein when primed through the T cell receptor (TCR) stimulation and that Tip60 deficiency leads to reduced Foxp3 expression and impaired both Treg differentiation and the suppression capability of Tregs in RA T cells. Mechanistic studies indicated that Tip60-regulated Foxp3 protein acetylation is critical for Foxp3 stability. Knockdown of the *Tip60* gene and the use of Tip60 acetyltransferase activity inhibitor reduced Foxp3 expression and Treg production during T cell differentiation, and impaired the suppression effects of Tregs. Ectopically expressed Tip60 recovered Treg differentiation and the suppression capability of Tregs in RA through elevation of acetylated Foxp3. Moreover, a deficiency in acetyltransferase activity of Tip60 has a significant impact on T cell tissue infiltration and renders T cells arthritogenesis, whereas restoration of Tip60 in $CD45RO^-$ peripheral blood mononuclear cells (PBMCs) attenuated the inflammatory state of the synovial tissue in a synovial tissue-engrafted humanized mouse model. Thus, Tip60 is critically involved in maintaining the differentiation balance and immune tolerance in proliferating $CD4^+$ T cells. Tip60-Foxp3 impairment in RA T cells may create an inflammation-prone T cell pool and induce a hyperinflammatory phenotype in the synovial tissue.

2. Materials and methods

2.1. Patients and control individuals

The study group included 89 individuals with a diagnosis of RA, 16 with knee osteoarthritis (OA), and 85 healthy controls (HCs). The RA patients fulfilled the American College of Rheumatology (ACR) criteria [32], and all RA patients were positive for rheumatoid factor and/or anticyclic citrullinated peptide antibody. The control subjects were matched with age, gender and ethnicity. A history of cancer, uncontrolled medical disease or any other inflammatory syndrome were excluded. Healthy individuals didn't have any personal or family history of autoimmune disease. The demographic characteristics of the OA and RA patients and HC donors are summarized in Table I. The study was approved by the Medical Ethics Committee of Hospital and all subjects provided appropriate informed consent.

Table 1
Demographic characteristics of the study populations.

Characteristics	HC	OA	RA	*P*
Demographic				
Number of subjects	85	16		89
Female/Male[a]	58/27	14/2	62/27	0.83
Age (mean ± SEM years)[a]	51.9 ± 1.6	54.8 ± 2.7	53.7 ± 1.8	0.21
Clinical characteristics				
Disease duration (mean ± SEM years)		N/A	8.1 ± 1.0	
Active disease		N/A	84.3%	
Tobacco use		N/A	22.5%	
Extra-articular manifestations		N/A	41.6%	
ESR, mm/h		N/A	39.5 ± 1.9	
DMARD naïve		N/A	10.1%	
Medications				
Corticosteroids		N/A	70.8%	
Methotrexate		N/A	67.4%	
Hydroxychloroquine		N/A	56.2%	
Leflunomide		N/A	24.7%	
TNF-α inhibitors		N/A	14.6%	

[a] No significant difference, RA patients compared with HC donors. ESR, erythrocyte sedimentation rate; DMARD, disease-modifying antirheumatic drugs; an active disease defined by Food and Drug Administration (FDA) criteria [presence of three or more of the following: morning stiffness (> 45 min), swollen joints (> 3), tender joints (> 6) and sedimentation rate (> 20 mm/h)].

2.2. Cell purification and culture

PBMCs from the whole blood were separated with Lymphocyte Separation Medium (Mediatech, Inc., Herndon, VA, USA). Synovial fluids (SFs) were collected from knee joints. The samples were centrifuged at 500 × *g* for 6 min. The pellets were diluted with PBS and filtered through 70 μm nylon filter. To sort $CD4^+CD45RO^-$ cells, PBMCs were negatively selected with CD45RO microbeads (Miltenyi Biotec Inc., Auburn, CA, USA), followed by positive selection with CD4 microbeads using autoMACS (Miltenyi Biotec Inc., Auburn, CA, USA).

$CD4^+CD45RO^-$ cells (1.0×10^5/well) were stimulated with CD3/CD28-coupled beads (Invitrogen, Carlsbad, CA, USA) in a 2.5:1 ratio. IL-2 (20 IU/ml) was added on days 0 and 3. The cells were counted by flow cytometry or trypan blue exclusion.

For T cell differentiation, $CD4^+CD45RO^-$ T cells (1.0×10^5/well) were seeded into U-bottomed 96-well plates pre-coated with anti-CD3 (1 μg/ml; BioLegend, USA) and anti-CD28 (1 μg/ml; BioLegend, USA). Tregs differentiation: IL-2 (10 U/ml), TGF-β1 (2.5 ng/ml) and neutralizing antibodies to IL-4 (1 μg/ml) and IFN-γ (1 μg/ml) were added. Th17 cell differentiation: IL-1β (10 ng/ml), IL-6 (10 ng/ml), IL-21 (10 ng/ml), IL-23 (10 ng/ml), TGF-β1 (2.5 ng/ml) and neutralizing antibodies to IL-4 (1 μg/ml) and IFN-γ (1 μg/ml) were added. All cytokines were obtained from Peprotech (Peprotech, Rocky Hill, NJ, USA). The cells were collected on day 6 and analyzed by flow cytometry.

Suppression assays for Tregs were performed by culturing CFSE-labeled naïve $CD4^+CD25^-$ T cells (responder cells) and $CD4^+CD25^+$ T cells (Tregs). $CD4^+CD25^+$ Tregs and $CD4^+CD25^-$ responder cells were isolated with Treg isolation kit (Miltenyi Biotec Inc., Germany), mixed, and seeded in round-bottom 96-well plates with 1:1 ratio. The cells were then stimulated with anti-CD3/CD28-coupled beads. After four days, the cells were stained with CD4-APC and PE-CD25 to discriminate each T-cell population and the proliferation of $CD4^+CD25^-$ T cells was detected as the dilution of CFSE on flow cytometry.

2.3. Flow cytometry

For intracellular staining, the cells were surface stained with FITC-CD4, APC-CD4, PE-CD4, PerCP-CD25 and PE-CD25 antibodies. Then, intracellular staining was performed with a BD Permeabilization/

Table 2
Primer sequences.

TIP60	5′-CGTAAGAACAAGAGTTATTCCCA -3′
	5′-GTCTTCCGTTGATTCTTTCTCC -3′
Foxp3	5'-CAGCCATGATCAGCCTCACA-3'
	5'-CACTGGGATTTGGGAAGGTG-3'
IL-6	5′-GGTACATCCTCGACGGCATCT-3′
	5′-GTGCCTCTTTGCTGCTTTCAC-3′
TNF-α	5′-TCTTCTCGAACCCCGAGTGA-3′
	5′-CCTCTGATGGCACCACCAG-3′
IL-17	5′-TCAACCCGATTGTCCACCAT-3′
	5′-AGTTTAGTCCGAAATGAGGCTG-3′
IL-10	5′-CCGAGATGCCTTCAGCAGAG-3′
	5′-GGTCTTGGTTCTCAGCTTGG-3′
TGFβ	5′-CCCAGCATCTGCAAAGCTC-3′
	5′-GTCAATGTACAGCTGCCGCA-3′
TRB	5'-CCTTCAACAACAGCATTATTCCAG-3'
	5'-CGAGGGAGCACAGGCTGTCTT-3'
TNFSF11	5′-CCCATAAAGTGAGTCTGTCC-3′
	5′-CAATACTTGGTGCTTCCTCC-3′
GAPDH	5′-GGTGGTCTCCTCTGACTTCAACA-3′
	5′-GTTGCTGTAGCCAAATTCGTTGT-3′

Fixation kit. A total of 10^7 cells/ml were stained with APC-IL-17a, FITC-IL-17a, FITC-Foxp3 and PE-Foxp3 antibodies. All antibodies were obtained from eBioscience (eBioscience, San Diego, CA, USA). The protein expression levels were detected by an LSRII flow cytometer (BD Biosciences, San Jose, CA, USA**)**. The data were analyzed with the FlowJo software.

2.4. RNA isolation and quantitative real-time PCR (QPCR)

Total RNA was extracted from 1.0×10^5 cells, and cDNA was synthesized with the AMV-reverse transcriptase and random hexamer primers (Roche Diagnostic Corp., Indianapolis, USA). Reverse transcription was performed using a standard procedure (Super Script First-Strand Synthesis System; Invitrogen) using 1 μg of total RNA. QPCR was performed using the iQ SYBR Green Supermix on the iCycler Real-Time Detection system (Bio-Rad, Hercules, CA, USA) [33]. The primer sequences used to amplify *Tip60*, *Foxp3*, *IL-6*, *TNF-α*, *IL-17*, *IL-10*, *TGF-β*, *TRB*, *TNFSF11* and *GAPDH* were listed in Table II. The relative amount of mRNA was normalized to that of the housekeeping *GAPDH* as indicated and then quantified.

2.5. Immunoprecipitation and western blotting

$CD4^+$ T cells were washed twice with cold PBS and lysed in 1.5 ml of cold lysis buffer (50 mM Tris-HCl, pH 7.6, 150 mM NaCl, 0.1% Triton X-100, 1 mM sodium orthovanadate, 1 mM sodium fluoride, 1 mM sodium pyrophosphate, 10 mg/ml aprotinin, 10 mg/ml leupeptin, 2 mM phenylmethylsulphonyl fluoride and 1 mM EDTA) on ice. The supernatants of the cell lysates were precleared by incubation with protein A/G PLUS-Agarose for 2 h. Then, the lysates were incubated with anti-Foxp3 (Santa Cruz Biotechnology, Santa Cruz, CA, USA) and protein A/G PLUS-Agarose on a rotator at 4 °C overnight. Immune complexes were collected after each immunoprecipitation by centrifugation at $13{,}000 \times g$ for 10 min, followed by washes with lysis buffer. The immune complexes were subjected to sodium dodecyl sulfate–polyacrylamide gel electrophoresis (SDS-PAGE), followed by immunoblotting with anti-Acetylated-Lysine Ac-K-103 (Cell signaling Technology, Danvers, MA, USA) and Foxp3-specific antibodies.

Our previously reported methods were applied for western blotting [5]. Briefly, whole-cell lysates were prepared in radioimmunoprecipitation (RIPA) buffer (Cell Signaling Technology, USA). Equal amounts of total protein from each sample were loaded into a SDS-PAGE gel and then transferred to a nitrocellulose membrane (Amersham, Piscataway, NJ, USA). Antibodies specific for Tip60 (Santa Cruz Biotechnology, USA), Foxp3 (Santa Cruz Biotechnology, USA) and acetylated-lysine Ac-K-103 (Cell signaling Technology, USA) were added, and the blots were incubated overnight at 4 °C. The membranes were subsequently incubated with secondary antibodies (1:5000; Santa Cruz, USA) for 1 h at room temperature and developed with a chemiluminescent detection system (GE Healthcare, Buckinghamshire, UK). To ensure equal loading, the membranes were stripped and reprobed for GAPDH using mouse anti-human GAPDH antibodies (1:4000; Santa Cruz Biotechnology).

2.6. shRNA-mediated knockdown

To knockdown Tip60 expression, four different *Tip60* shRNA-specific constructs with EGFP tags were synthesized with psi-U6-EGFP as the control vector (GeneCopoeia, Rockville, MD). Alternatively, Oligo duplex RNA specific for *Tip60* and a control siRNA were purchased from Santa Cruz Biotechnology (Santa Cruz, USA). 6 μg of siRNA oligonucleotides or shRNA constructs were transfected into purified $CD4^+$ T cells using the Amaxa Nucleofector system and the Human T Cell Nucleofector kit (Lonza Walkersville Inc., Walkersville, MD, USA) as previously described [5,9]. Twenty-four hours after transfection, the cell numbers were adjusted, and the $CD4^+$ T cells were stimulated as described above.

2.7. Transfection of Tip60 into naïve $CD4^+$ T cells

Naïve $CD4^+$ T cells were stimulated with anti-CD3/CD28 and transfected with pEGFP-C2 or pEGFP–Tip60; and pcDNA3.1 or pcDNA3.1-Tip60 using the Amaxa Nucleofector system and the Human T Cell Nucleofector kit (Lonza Walkersville Inc., USA). After 48 h, the transfection efficiencies were monitored by measuring the frequency of GFP-positive cells using a flow cytometer.

2.8. Synovitis induction in chimeric mice

Female NOD.Cg-PrkdcscidIl2rgtm1 Wjl/SzJ (NSG) mice (10–14 weeks old) (The Jackson Laboratory, Bar Harbor, ME, USA) were used as previously described [34]. Pieces of synovial tissue from RA patients were placed into a subcutaneous pocket on the upper dorsal midline. For the inhibitor experiment, following engraftment, the mice were injected intravenously with 10 million $CD45RO^-$ PBMCs which separated from healthy controls. Chimeric mice from the same litter and carrying the same synovial tissue were randomly assigned to two groups: either treated with vehicle (DMSO) control or treated with Tip60 inhibitor NU9056, 2 mg/kg/day. Both treatments were delivered by daily intraperitoneal injection over a period of 9 days. For the Tip60 overexpression, chimeric mice from the same litter that carried the same synovial tissue were randomly assigned to two groups. $CD45RO^-$ PBMCs were prepared from RA patients and transfected with either a control plasmid (pCDNA3.1) or a pCDNA3.1-Tip60 plasmid. The transfected cells were rested for 24 h before adoptive transfer. At the end of the experiments, the mice were sacrificed, and the synovial tissues were harvested and embedded in paraffin for histological studies or shock frozen in liquid nitrogen for RNA extraction [35].

2.9. Synovial histopathological examination and immunostaining

Paraffin-embedded synovial tissues were sectioned continuously at 5 mm intervals, and the sections were subjected to standard haematoxylin and eosin (H&E) staining or stained using FITC-IL-17a (eBioscience, USA), FITC-Foxp3 (eBioscience, USA), anti-CD3 (Abcam, USA), anti-CD20 (Invitrogen, Carlsbad, CA, USA), anti-RANKL (Abcam, Cambridge, MA, USA), anti-Tip60 (Santa Cruz, USA) and acetylated-lysine Ac-K-103 (Abcam), followed by an staining with horseradish peroxidase (HRP)-conjugated or fluoresce-conjugated second antibodies per standard staining protocols. Isotype-matched primary antibodies served as controls. Antibody binding was examined by light

microscopy or fluorescence microscopy. Positive-staining cells were determined by manual counting observing 9 different fields of synovial tissue sections at magnification of ×400 as we previously reported [36]. As one area of 400× magnification revealed a synovial area of 0.11740 mm^2, nine microscopy fields reveal an area of nearly 1 mm^2 which is proved to be representative.

2.10. Statistical analysis

Groups were compared using parametric *t*-tests for independent or paired samples as appropriate. The results were expressed as the mean ± standard error of the mean (SEM). The Chi-square test was used to compare categorical variables between different groups. *P* values less than 0.05 were considered significant.

3. Results

3.1. Reduced Treg production in RA patients

Tregs play a critical role in protecting the onset of RA by suppressing inflammation. To verify the Treg and Th17 cell production under autoimmune inflammatory conditions, the frequencies of $CD4^+CD25^+Foxp3^+$ Tregs and $CD4^+IL\text{-}17^+$ Th17 cells were examined in PBMCs and SFs from RA patients using flow cytometry. To exclude factors that impact T cell differentiation other than immune regulation, the frequency of Tregs and Th17 cells was also detected in matched OA patients; OA was used as the disease control, as it is characterized by cartilage damage induced by abnormal wearing of the cartilage and low inflammation. Compared with the OA patients, the frequency of $CD4^+CD25^+Foxp3^+$ Tregs in RA patients was significantly lower both among PBMCs (1.54% vs. 0.47%, $P = 0.0005$; Fig. 1A and B) and in the SFs (2.38% vs. 1.33%, $P = 0.003$; Fig. 1A and B), whereas the frequency of IL-17-producing $CD4^+IL\text{-}17^+$ Th17 cells in RA patients was significantly higher both among PBMCs (0.75% vs. 3.5%, $P = 0.0008$; Fig. 1C and D) and in the SFs (0.97% vs. 5.7%, $P = 0.0009$; Fig. 1C and D), indicating an immune imbalance between Tregs and Th17 cells occurred in RA disease. Consistently, the synovium from RA patients contained significantly higher levels of Th17-associated cytokines, including *IL-17, TNF-α* and *IL-6*, and lower levels of *IL-10* and *TGF-β*, which are Treg cytokines that inhibit inflammation in tissues (Fig. 1E). These data strongly suggested that synovial arthritis in RA patients is dominated by a Treg/Th17-based mechanism.

To determine whether maldifferentiation of Tregs and Th17 cells was relevant in RA, the naïve $CD4^+$ T cells from RA patients and matched HCs and OA patients were polarized under Treg- and Th17-polarizing conditions. Under Treg-polarizing conditions, there was an evidently lower frequency of ($CD4^+CD25^+Foxp3^+$) in RA T cells after introduction, namely 4.5% compared with 14.3% in OA and 15.7% in HCs. Under Th17-polarizing conditions, the RA T cells were tended to commit to the Th17 differentiation program, with a frequency of Th17 cells ($CD4^+IL17^+$) of 25.1% in RA patients as opposed to the 6.8% in OA and 5.0% in HCs (Fig. 1F and G). Moreover, the suppression capacity of Tregs from HCs, OA and RA patients were determined by conculturing Tregs with CFSE-labeled naïve $CD4^+$ T cells, and the suppression efficiency was calculated by the rate of CFSE dilution. $CD4^+$ T cells were more susceptible to the suppressive effects of Tregs from HCs and OA patients than of Tregs from RA patients with the division indices being (HC, 1; OA, 1.16; and RA, 1.62) (Fig. 1H and I). These results suggested that the Tregs differentiation program and Treg suppression efficiency are blocked in RA patients.

3.2. Naïve $CD4^+$ T cells from RA patients fail to induce Foxp3

The insufficient differentiation of Tregs from RA T cells raised the question of whether Foxp3, the key transcription factor for Treg differentiation, was functional. To assess Foxp3 expression in naïve $CD4^+$ T cells, T cells marked with $CD4^+CD45RO^-$ were purified from PBMCs collected from RA patients and matched HCs and OA patients. The cells were activated with anti-CD3/CD28. Both gene and protein expression levels of Foxp3 were evaluated to identify the underlying mechanism of Foxp3 deficiency. As shown in Fig. 2, The abundance of *Foxp3* mRNA in naïve $CD4^+$ T cells from RA patients was comparable to that in naïve $CD4^+$ T cells from HCs and OA patients (Fig. 2A). The reduced Foxp3 expression in RA T cells was confirmed by flow cytometry, which showed a reduction of nearly 50% in the FITC-Foxp3 mean fluorescence intensity (MFI) in RA patients compared with the MFI in HCs and OA patients (Fig. 2B and C). However, the results of western blotting revealed significantly decreased Foxp3 levels in naïve T cells from RA patients, whereas increased levels were observed in T cell populations from both HCs and the OA patients (Fig. 2D). These results suggested that the Foxp3 downregulation in RA T cells is associated with the post-translational modification mechanisms.

Since acetylation is a key protein modification for maintaining the stability of Foxp3, the Foxp3 acetylation level was measured by immunoprecipitation assay using a Foxp3 antibody and subsequent western blotting with an anti-acetylated-lysine antibody. A substantially lower level of acetylated-Foxp3 level was found in the RA T cells than T cells of HCs and OA patients when loading same amounts of Foxp3 protein for all three groups, indicating a deficiency of Foxp3 acetylation occurring in the RA T cells after priming (Fig. 2E and F).

3.3. RA T cells fail to upregulate the Tip60 acetyltransferase during activation

Tip60 is the key acetyltransferase in Foxp3 acetylation, and Tip60-mediated Foxp3 acetylation protects Foxp3 from protein degradation and subsequently promotes Treg differentiation [30]. To assess whether the loss of Foxp3 acetylation in RA patients was caused by Tip60 deficiency, Tip60 induction during priming was examined. The $CD4^+CD45RO^-$ cell population was stimulated with anti-CD3/CD28 beads, Transcript levels of *Tip60* were detected in the naïve CD4 T cells from RA patients and age-matched HCs and OA patients. There was a significantly lower of *Tip60* expression in the naïve T cells of RA than that from HCs and OA patients (Fig. 3A and B). To assess the impact of immunosuppressive therapy and the disease state on Tip60 induction, we examined the newly diagnosed RA patients that were not on disease-modifying anti-rheumatic drugs (DMARDs) treatment or corticosteroid treatment within three months before the samples were collected. We found no significant difference between the *Tip60* levels in the treated and untreated patients (Fig. 3C), which excluded drugs as the sole causative factors underlying *Tip60* insufficiency. Remarkably, the decreased *Tip60* expression was significantly correlated with reduced Tregs production in individual T cell samples from RA patients (Fig. 3D). To confirm that the co-occurred downregulation of Tip60 and Foxp3 in RA patients, their protein expression in HCs, OA and RA T cells were quantified by western blotting. The results showed that both the Tip60 and Foxp3 band intensities were significantly downregulated in RA $CD4^+$ T cells compared with the intensities of HCs and OA (Fig. 3E and F).

To assess the correlation of insufficient Tip60 expression with impaired Foxp3 expression, Total nuclear Tip60 and Foxp3 expression were visualized by dual-color immunostaining with anti-Tip60 and anti-Foxp3 antibodies. Elevated expression of Tip60 and Foxp3 under stimulation were found and these elevations were highly efficient in healthy T cells. There was a clear Tip60 and Foxp3 colocalization signal with yellow color observed in this cell type. In contrast, both the Tip60 and Foxp3 nuclear signals were markedly lower in the RA-derived T cells (suppl. Fig. 1A and B). Moreover, to explore the pathogenic roles of the Tip60 regulated foxp3 acetylation in the synovitis of RA patients, synovial sections from OA and RA patients were staining with Foxp3, acetylated-lysine, and Tip60 antibodies. We observed that the expression of Foxp3 and acetylated-Foxp3 and Tip60 was absent in sections

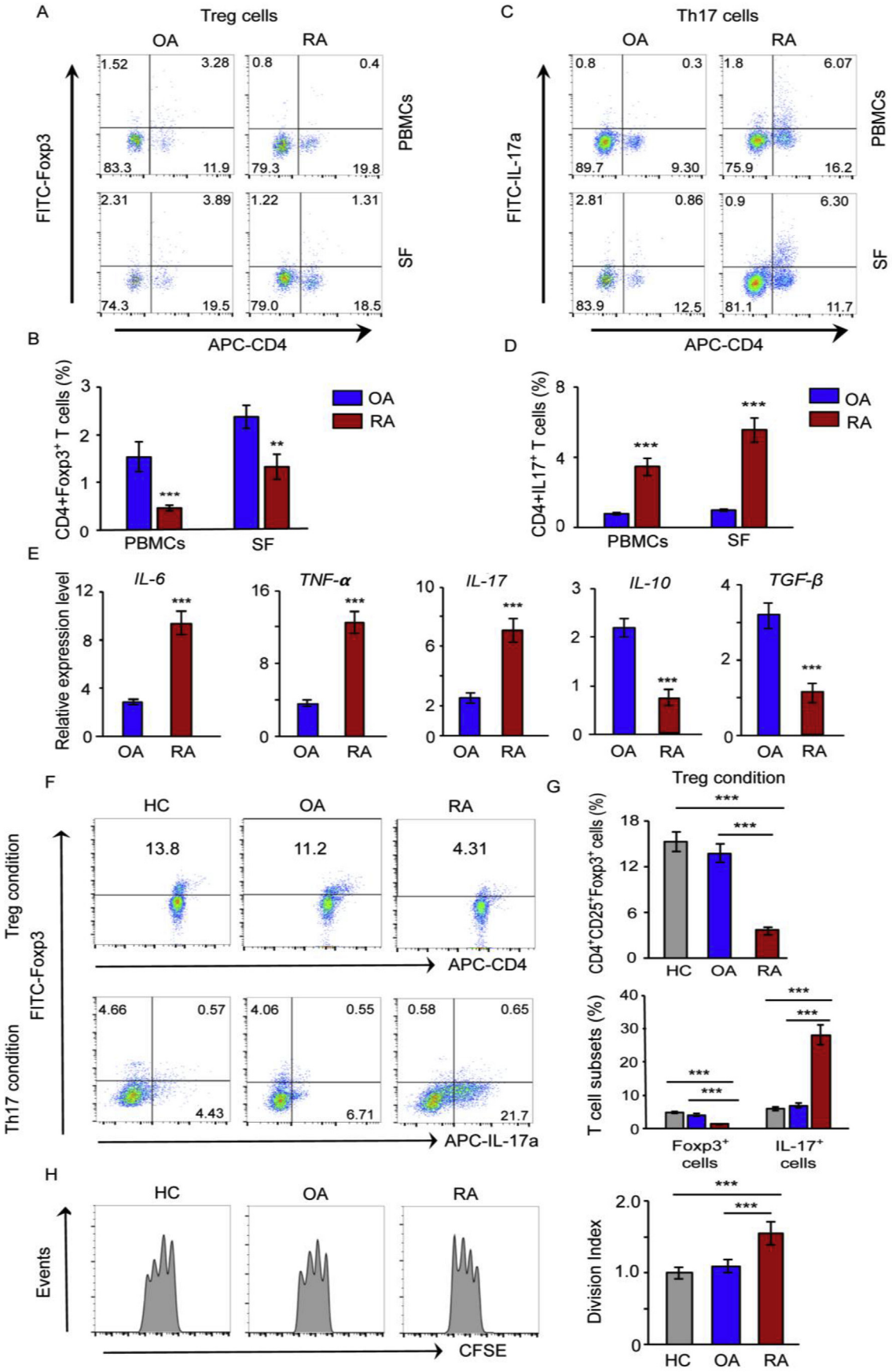

(caption on next page)

Fig. 1. Deficiency of Treg cell differentiation in RA patients. (A–D) T cell subsets among PBMCs and in the SFs were isolated from RA (n = 6) and OA patients (n = 6). (A–B) Treg cell subsets: cells were stained with antibodies against CD4, CD25, and Foxp3. (A) Representative dot plots. (B) Percentages of $CD4^+CD25^+Foxp3^+$ cells among PBMCs and in the SFs from 3 experiments examining 6 RA patients and 6 OA patients are presented as the mean ± SEM. (C–D) Th17 cell subsets: cells were stained with antibodies against CD4 and IL-17a. (C) Representative dot plots. (D) Percentages of $CD4^+IL\text{-}17^+$ cells among PBMCs and in the SFs from 3 experiments examining 6 RA patients and 6 OA patients are presented as the mean ± SEM. (E) Production of cytokines *IL-6*, *TNF-α*, *IL-17*, *IL-10* and *TGF-β* in the synovium was measured by QPCR. The data are representative of three independent experiments. (F–G) T cell differentiation: $CD4^+CD45RO^-$ T cells were cultured under Treg-polarizing or Th17-polarizing conditions, restimulated with PMA/ionomycin, and stained to evaluate intracellular Foxp3 and IL-17a expression. (F) Representative dot plots for Treg cell (right) and Th17 cell (left) production. (G) Percentages of Tregs ($CD4^+CD25^+Foxp3^+$) under Treg-polarizing conditions or $CD4^+Foxp3^+$ Tregs and $CD4^+IL\text{-}17a^+$ Th17 cells under Th17-polarizing conditions from 3 experiments examining 10 RA patients, 10 OA patients, and 10 healthy controls (HCs) are presented as the mean ± SEM. (H-I)$CD4^+CD25^+$ Tregs were generated from HCs, OA and RA patients. On day 6, Tregs were purified and cocultured at a 1:1 ratio with CFSE-labeled $CD4^+CD25^-$ cells. Cocultures were stimulated with anti-CD3/CD28 beads. On day 4 of the coculture, proliferation of the $CD4^+$ T cells was analyzed by quantifying CFSE dilution using flow cytometry. (H) Histograms from a representative experiment are shown. (I) The mean ± SEM of CFSE division of $CD4^+$ T cells are shown for 6 independent experiments. $^{**}P < 0.01$; $^{***}P < 0.001$.

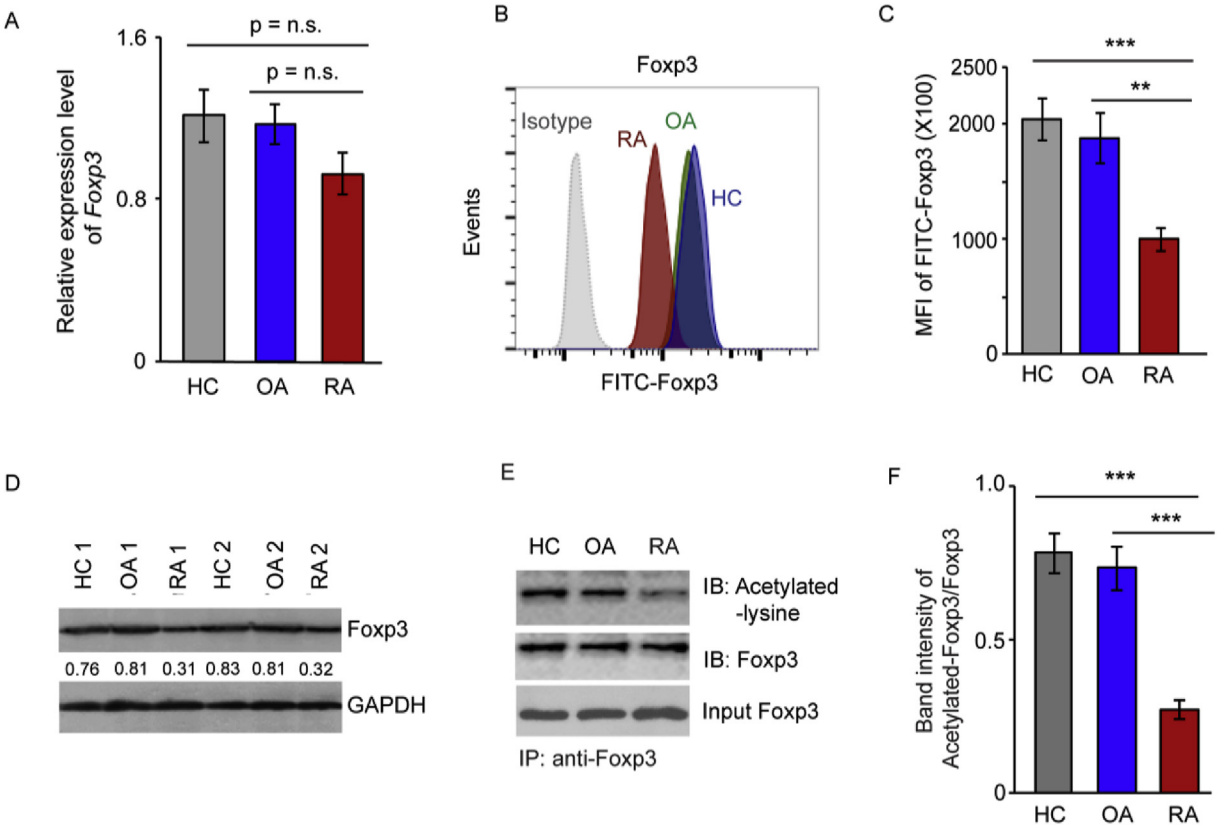

Fig. 2. Low Foxp3 expression in naïve T cells from RA patients. $CD4^+CD45RO^-$ T cells from RA, OA patients and matched HCs were stimulated for 4 days. (A) The *Foxp3* transcript levels were quantified by QPCR. The mean ± SEM of three experiments is shown. (B) Foxp3 protein level in naïve T cells was analyzed by flow cytometry. The FITC-Foxp3 MFIs from representative histograms for one HC (blue), one OA, and one RA (red) patient are shown. The isotype control (IgG) is superimposed as a shaded area. (C) Three independent experiments examining 10 RA patients, 10 OA patients, and 10 HCs are presented as the mean ± SEM. (D) Foxp3 protein expression was detected by western blotting. The Foxp3 band intensities were normalized to GAPDH. The images are representative of 3 independent experiments with 10 RA patients, 10 OA patients, and 10 HCs. (E–F) Insufficient protein acetylation of Foxp3: (E) after adjusting the cell lysates from HCs and OA and RA patients with same amounts of Foxp3 protein, acetylated-Foxp3 level was determined with using a coimmunoprecipitation assay with anti-Foxp3, followed by immunoblotting with anti-acetylated-lysine and anti-Foxp3 antibodies. Representative blots from three independent experiments are shown. (F) The band intensity of acetylated-Foxp3 was normalized to Foxp3. The coimmunoprecipitation experiment results analyzing 6 RA patients, 6 OA patients and 6 HCs are shown as the mean ± SEM. $^{**}P < 0.01$; $^{***}P < 0.001$; n.s., non-significance. (For interpretation of the references to color in this figure legend, the reader is referred to the Web version of this article.)

from RA patients but stronger in OA patients. Moreover, three staining show similar decreasing tendency of Foxp3, acetylated-Foxp3 and Tip60 expression in RA synovium when compared with OA (Fig. 3G and H).

3.4. *Tip60* activity inhibition or silencing impairs *Foxp3* expression and Treg differentiation

To assess whether diminished Tip60 contributes to the tissue infiltration and pro-inflammatory effect of RA T cells, *Tip60* gene expression in naïve $CD4^+$ T cells was inhibited using a *Tip60* siRNA (Fig. 4). Twenty-four hours later, the T cells were stimulated with anti-CD3/CD28-beads. *Tip60* sequence-specific knock down significantly reduced the *Tip60* gene and Tip60 protein expression (Fig. 4A and B), which mimicked the conditions in RA T cells. Impaired Tip60 induction in T cells also downregulated the level of the Foxp3 acetylation in the healthy T cells to the level observed in the RA T cells (Fig. 4C). To further clarified that Tip60 downregulation reduce Foxp3 expression, we made GFP tagged *Tip60* shRNA. Flow cytometry showed that 25%–40% of the T cells transfected with either the psi-U6-EGFP or psi-

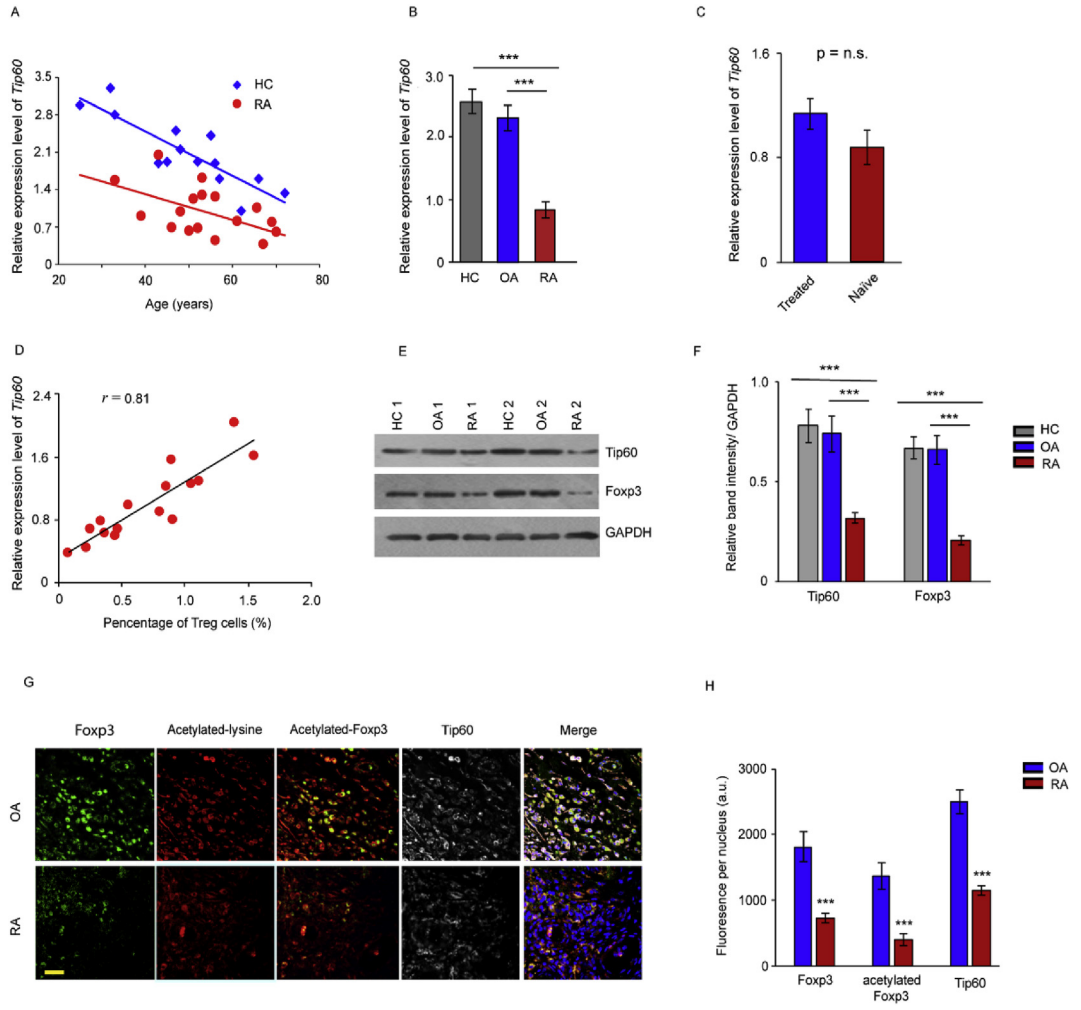

Fig. 3. Impaired Tip60 expression in RA patients. $CD4^+CD45RO^-$ T cells from RA patients and controls were stimulated for 4 days, and (A–B) *Tip60* gene expression was quantified by QPCR in naïve T cells from RA patients, HCs and OA patients. The results from 3 independent experiments involving 16 RA patients and 14 HCs are shown as scatter plots in relation to the donor age (A) and as bar graphs displaying the mean ± SEM of the RA patients, HCs and OA patients (B). (C) *Tip60* insufficiency is independent of drug treatment (treated vs. treatment naïve), and *Tip60* gene expression was measured in the naïve $CD4^+$ T cells 4 days after TCR-mediated stimulation. (D) *Tip60* transcript levels were correlated with the number of Treg cells in the PBMCs from RA patients. (E–F) Representative blotting for Tip60 and Foxp3 protein expression (E). The Tip60 and Foxp3 band intensities were adjusted to GAPDH. The western blotting experiment results analyzing 6 RA patients, 6 OA and 6 HCs are shown as the mean ± SEM (F). (G) Co-immunostaining of Foxp3 (green), acetylated-lysine (red), and Tip60 (white). Representative images are from one of three synovial tissue sections from the OA and RA patients. Bar, 20 μm. (H) Fluorescence intensities of Foxp3 (green), acetylated-lysine (red), acetylated-Foxp3 (combined green and red), and Tip60 (white) in the sections of synovial tissue from 6 OA and 6 RA patients are presented as the mean ± SEM. ***$P < 0.001$; n.s., non-significance. (For interpretation of the references to color in this figure legend, the reader is referred to the Web version of this article.)

U6-EGFP-Tip60 vector were GFP^+ (suppl. Fig. 2A). The loss of Foxp3 acetylation was concomitant with reduced Foxp3 expression, as indicated by the flow cytometry assay after gating the GFP^+ cell population in control and *Tip60* shRNA-transfected cells (Fig. 4D and Suppl. Fig. 2B). Consistent with the decrease in the Tip60-Foxp3 axis, the production rate of Tregs was significantly lower in the *Tip60* siRNA-transfected cells than in the control siRNA-transfected cells. The frequency of Tregs decreased from 13.8% in the controls to 5.5% in the *Tip60*-deficient T cells, whereas the frequency of Th17 cells was increased from 6.2% in the controls to 25.6% in the *Tip60*-deficient T cells (Fig. 4E and F). Moreover, the suppression assays for *Tip60* siRNA-transfected and control siRNA-transfected Tregs indicated that the suppressive properties of the Tregs after *Tip60* knock down were much weaker than those of control Tregs (Fig. 4G). These results indicated that Tip60 expression is strongly correlated with Foxp3 expression and subsequent Treg differentiation.

In an alternative approach to assess the correlation of Tip60-regulated Foxp3 expression with the acetyltransferase activity of Tip60, T cells were treated with Tip60 inhibitor NU9056, which specifically inhibits Tip60-regulated protein acetylation. We observed that inhibition of the enzymatic activity of Tip60 induced a significant down-regulation of Foxp3 protein acetylation and expression and Treg differentiation. A 2 μM dose of NU9056 was sufficient to reduce Foxp3 expression (Fig. 4H–J) and Treg production to the levels seen in the RA T cells (Fig. 4K and L), which concomitant with the reduced suppression capability in Tregs with activity inhibition of Tip60 (Fig. 4M). Those data suggested that Tip60-dependent Foxp3 acetylation is essential for Foxp3 protein stability and Treg cell production.

3.5. Ectopic Tip60 expression rescues Foxp3 expression and Treg differentiation

To examine whether the reconstitution of *Tip60* expression could protect Foxp3 from degradation in RA T cells and rebuild Treg differentiation, pEGFP-Tip60 or control plasmids were transfected into purified $CD4^+$ T cell. The results showed that restoring adequate level of *Tip60* was sufficient to recover the acetylation defect of Foxp3 and repair Foxp3 expression in RA $CD4^+$ T cells, suggesting that Tip60 can

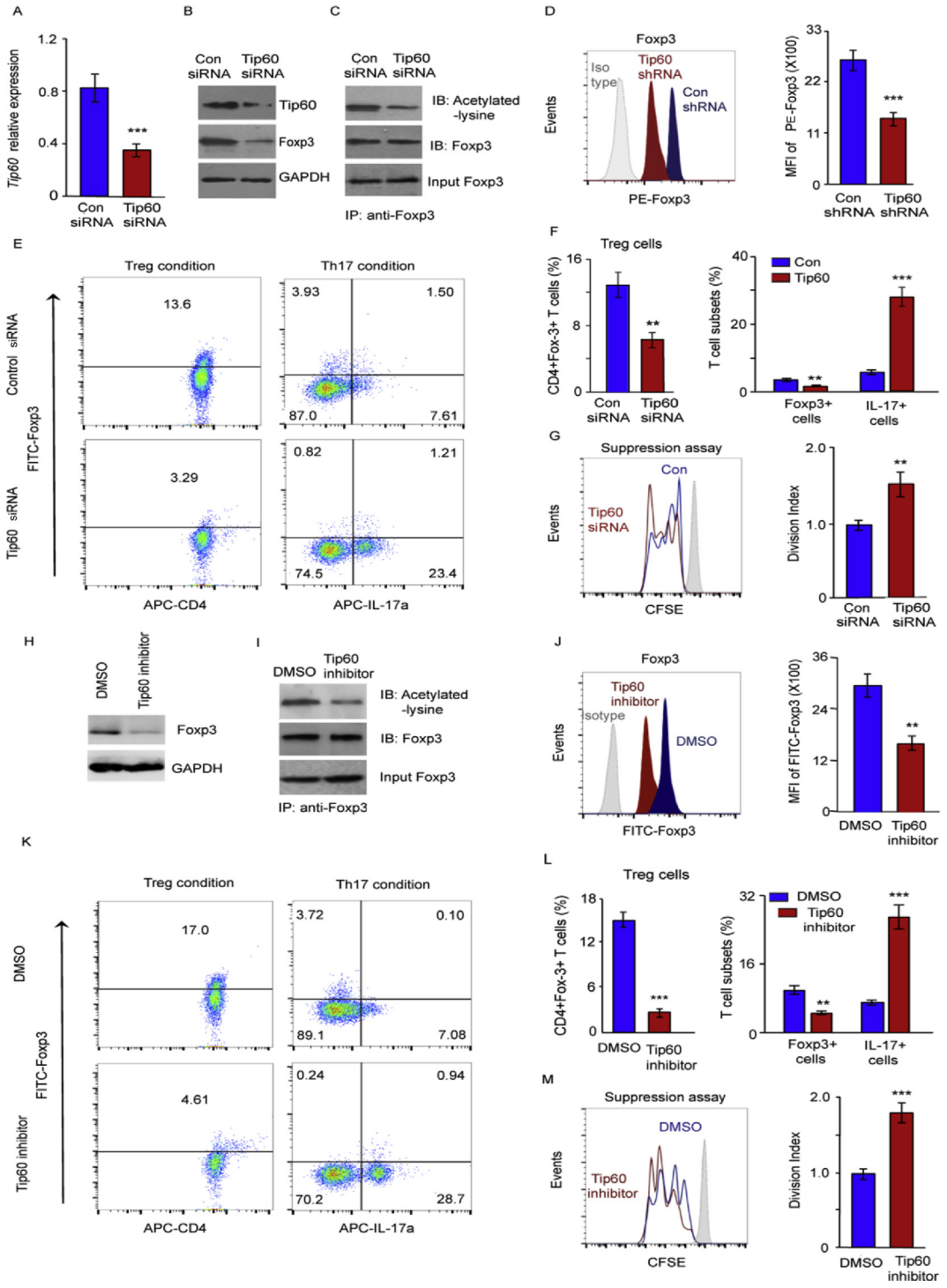

Fig. 4. Foxp3 expression and Treg cell differentiation are regulated by Tip60. $CD4^+$ T cells from healthy donors were transfected with control or Tip60-specific shRNA by nucleofection or treated with Tip60-specific inhibitor NU9056 (2 μM) at day 3 after bead stimulation. (A) The *Tip60* transcript levels were quantified by QPCR 24 h after control and *Tip60* siRNA transfection. (B) Representative blotting for Tip60 and Foxp3 expression. (C) Foxp3 acetylation was determined by a coimmunoprecipitation assay after transfection. (D) The Foxp3 levels in T cells were analyzed by flow cytometry in the GFP^+ cell population after control and *Tip60* shRNA transfection. Representative histograms for one control shRNA (blue) and one *Tip60* shRNA (red); three independent experiments examining 6 HCs are presented as the mean ± SEM. (E–G) $CD4^+$ T cells were transfected with the control or *Tip60* siRNA and cultured under Treg- or Th17-polarizing conditions, and intracellular staining for Foxp3 and IL-17a was performed. (E) Representative dot plots for Treg and Th17 cell production. (F) Percentages of Tregs under Treg-polarizing conditions or $CD4^+Foxp3^+$ cells and $CD4^+IL\text{-}17a^+$ Th17 cells under Th17-polarizing conditions are presented as the mean ± SEM. (G) Suppression ability of the Tregs from control and *Tip60* siRNA was analyzed by quantifying CFSE dilution. (H–M) Tip60 inhibitor: (H) Representative blotting for Foxp3 protein expression after NU9056 treatment. (I) Foxp3 acetylation was determined by a coimmunoprecipitation assay. (J) The Foxp3 protein levels in T cells were analyzed by flow cytometry. Representative histograms for DMSO (blue) and the Tip60 inhibitor (red); three independent experiments examining 6 HCs are presented as the mean ± SEM. (K–M) $CD4^+$ T cells were treated with vehicle (DMSO) or NU9056 (2 μM) and cultured under Treg- or Th17-polarizing conditions. (K) Representative dot plots. (L) Percentages of Tregs or Th17 cells are presented as the mean ± SEM. (M) Suppression ability of the Tregs from vehicle and inhibitor treatment cells was analyzed by quantifying CFSE dilution. $^{**}P < 0.01$; $^{***}P < 0.001$. (For interpretation of the references to color in this figure legend, the reader is referred to the Web version of this article.)

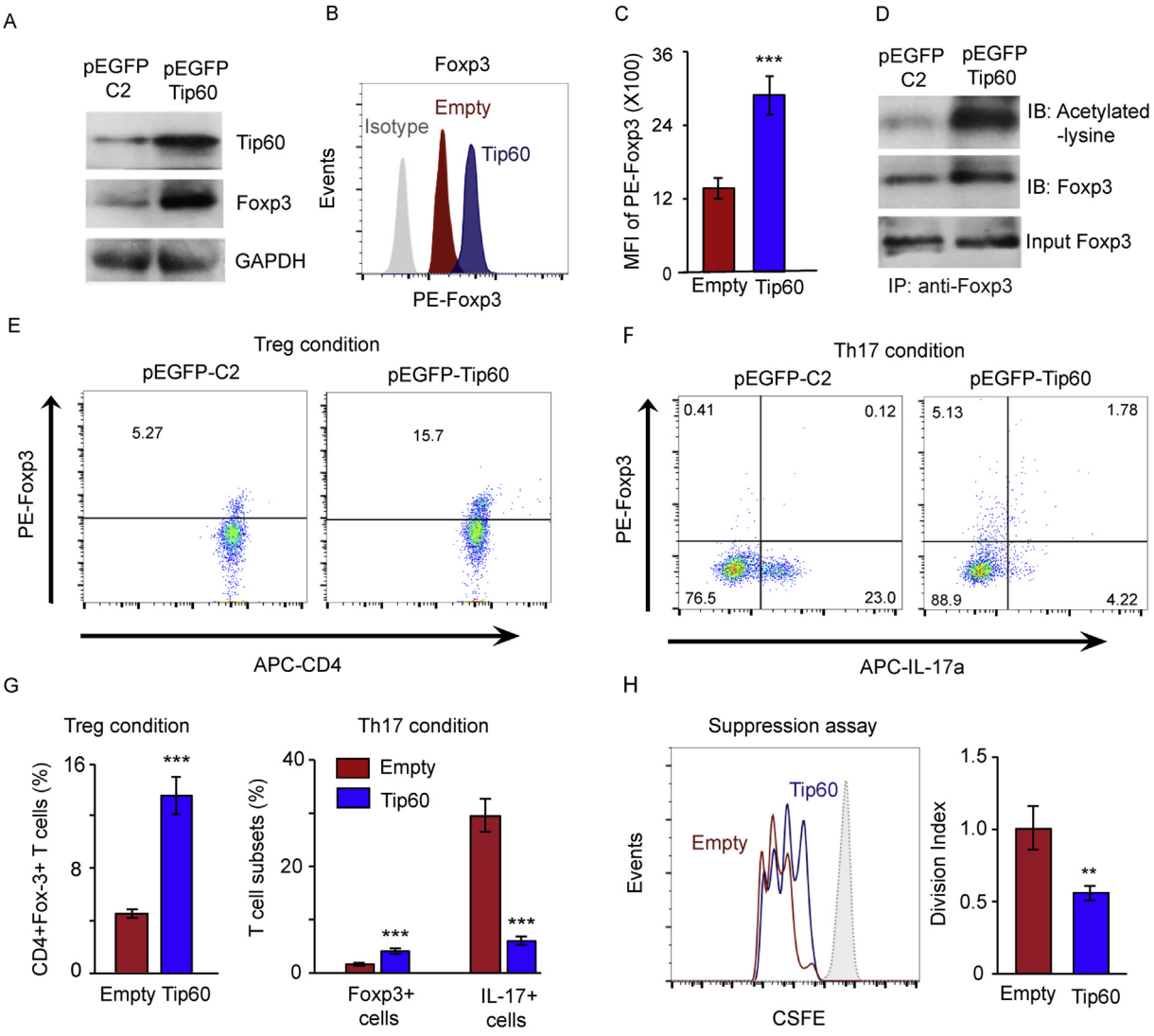

Fig. 5. Overexpression of Tip60 restores Treg cell differentiation. Naïve $CD4^+$ T cells from RA patients were transduced with pEGFP-C2 or pEGFP-Tip60. The cells were transfected after anti-CD3/CD28 bead stimulation. (A) Representative blotting for Tip60 and Foxp3 protein expression after transfection. (B–C) The Foxp3 protein levels in naïve T cells were analyzed by flow cytometry in GFP^+ cell population after transfection (B). Three independent experiments examining 6 RA patients are presented as the mean ± SEM (C). (D) Foxp3 acetylation was determined by a coimmunoprecipitation assay with anti-Foxp3, followed by immunoblotting with an anti-acetylated-lysine antibody. Representative blots from three independent experiments are shown. (E–H) T cell differentiation: $CD4^+CD45RO^-$ T cells were cultured under Treg- or Th17-polarizing conditions, re-stimulated with PMA/ionomycin and subjected to intracellular staining for Foxp3 and IL-17a. (E–F) Representative dot plots for Tregs (right) and Th17 cell (left) production. (G) Percentages of Tregs under Treg-polarizing condition or $CD4^+Foxp3^+$ cells and $CD4^+IL\text{-}17a^+$ Th17 cells under Th17-polarizing conditions from three independent experiments examining 6 RA patients are presented as the mean ± SEM. (H) Naïve $CD4^+$ T cells from RA patients were transduced with pcDNA3.1and pcDNA3.1-Tip60. Suppression capability of the Tregs from cells transfected with control and Tip60 plasmids was analyzed by quantifying the CFSE dilution. The mean ± SEM of division indics are shown from 6 independent coculture experiments. $^{**}P < 0.01$; $^{***}P < 0.001$.

stabilize Foxp3 expression through enhancing Foxp3 acetylation (Fig. 5A–D).

Direct quantification of Treg/Th17 cells in the transfected T cell populations revealed no significant difference of Foxp3 levels in the control vector-transfected T cells and the RA T cells. In contrast, RA T cells successfully transfected with the *Tip60* plasmid displayed a marked improvement of the Treg frequency concomitant with a decrease in Th17 frequency. The frequency of Tregs improved from 4.6% in cells transfected with the control vector to 13.8% in cells overexpressing *Tip60* (Fig. 5E, G), whereas the frequency of Th17 cells fell from 28.8% in cells transfected with the control vector to 6.3% in cells overexpressing *Tip60* (Fig. 5F and G). The suppressive capability of the Tregs after *Tip60* reconstitution was significantly elevated compared to the Tregs from control vector-transfected cells (Fig. 5H). These results directly indicate the role of Tip60-dependent Foxp3 acetylation in Treg differentiation.

3.6. Inhibition of Tip60 increases T cells tissue infiltration and proinflammatory effects

During T cell-mediated synovial inflammation, T cells need to gain infiltration activity and accumulate in the synovial tissue, where they exhibit arthritogenic effects by producing proinflammatory cytokines and activating other immune cells. To investigate the process through which T cells initiated and drive synovitis, we used a human-SCID chimeric mouse model in which the synovial tissue from RA patients was transplanted into the immunodeficient mice and the $CD45RO^-$ PBMCs from healthy donors were adoptively injected to the chimeric mice, and the mice were subsequently treated with the Tip60 inhibitor NU9056 (Fig. 6).

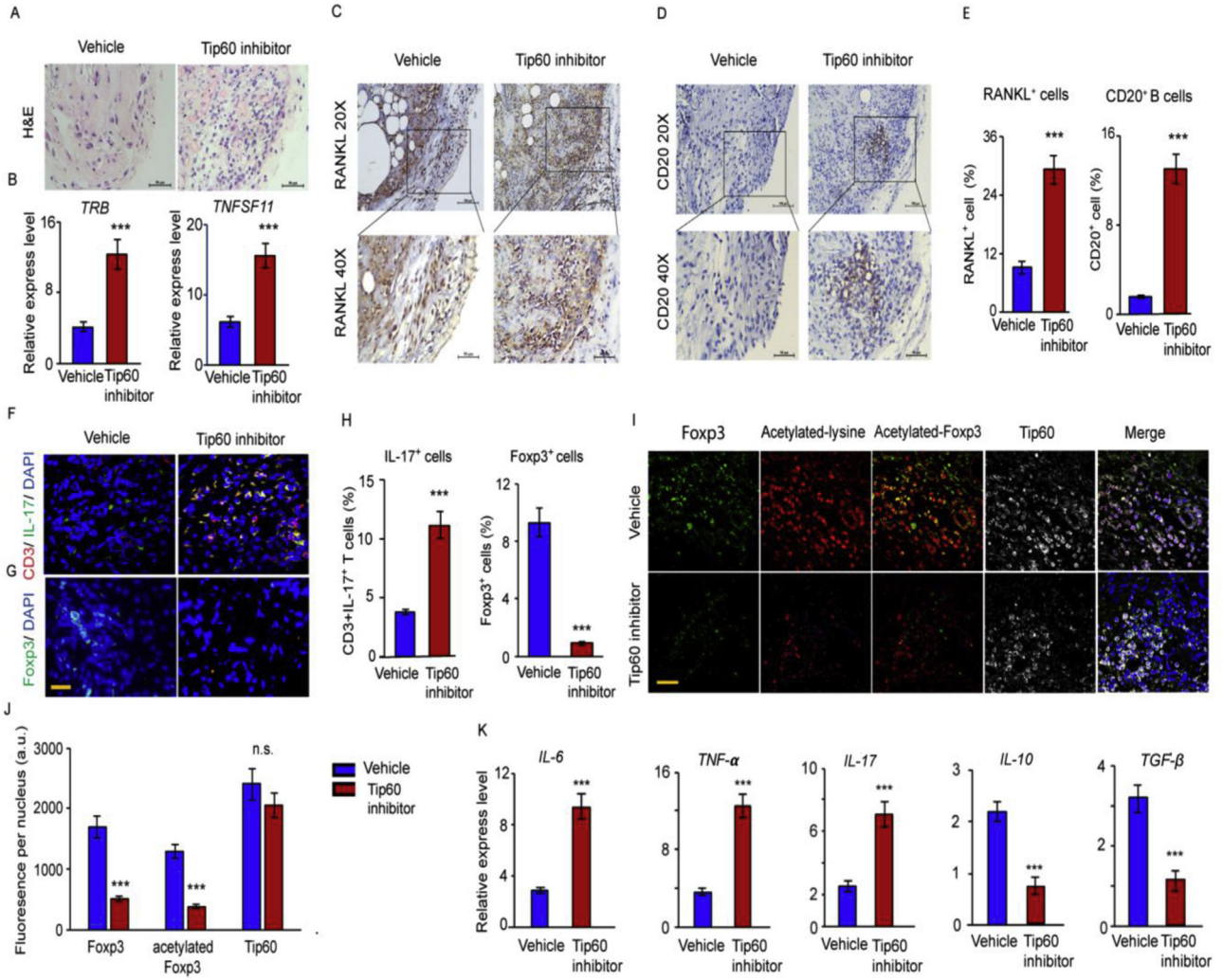

Fig. 6. Tip60 controls the arthritogenic effect of T cells. Pairs of NSG mice were engrafted with synovial tissue from RA patients, CD45RO$^-$ PBMCs from healthy donors were transferred to the chimeric mice. The mice were divided into two groups, vehicle (DMSO) control and treatment with NU9056 group, where both treatments were delivered by intraperitoneal injection of 2 mg/kg/day for 9 days. (A) H&E staining was performed to compare the overall morphology of the synovium. Representative images of the synovium in the vehicle (n = 6) and Tip60 inhibitor-treated (n = 6) chimeric mice are shown. The data are representative of three independent experiments. (B) The intensity of synovial inflammation was compared by QPCR to assess *TRB* and *TNFSF11* gene expression. All data are presented as the mean ± SEM from at least 6 different synovial grafts. (C–E) CD20 (C) and RANKL (D) were stained by immunohistochemistry in synovial tissue sections. The percentages of CD20$^+$ B cells and RANKL-positive cells were determined by counting 9 different fields of synovial tissue sections and presented as the mean ± SEM (E). (F–H) T cell infiltration: (F) Representative images of anti-CD3 (red) and IL-17a staining (green) of the vehicle- (n = 6) and Tip60 inhibitor-treated (n = 6) chimeric mice. CD3$^+$IL-17$^+$ double positive cells are indicated by a yellow coloring. Bar, 20 μm. (G) Representative images of anti-Foxp3 staining (green) of the vehicle- (n = 6) and Tip60 inhibitor-treated (n = 6) samples. Bar, 20 μm. (H) The percentages of CD3$^+$IL-17$^+$ cells and Foxp3$^+$ cells are presented as the mean ± SEM. (I) Co-immunostaining of Foxp3 (green), acetylated-lysine (red), and Tip60 (white). Representative images are from one of three synovial tissue from vehicle and Tip60 inhibitor-treated chimeric mice. Bar, 20 μm. (J) Fluorescence intensity of Foxp3, acetylated-Foxp3 (combined green and red) and Tip60 are presented as the mean ± SEM. (K) Expression of *IL-6*, *TNF-α*, *IL-17*, *IL-10* and *TGF-β* in the synovium was measured by QPCR. The data are representative of three independent experiments. ***$P < 0.001$; n.s., non-significance. (For interpretation of the references to color in this figure legend, the reader is referred to the Web version of this article.)

The inhibition of Tip60 acetyltransferase activity resulted in an enhanced tissue accumulation of immune cells, as indicated by H&E staining showing morphological changes (Fig. 6A). The inhibition of Tip60 activity significantly upregulated the gene expression of T cell receptor beta locus (*TRB*), which is indicative of an increase in T cell infiltration, and *TNFSF11* (encoding RANKL) transcription, which is a critical in mediating rheumatoid bone destruction (Fig. 6B) [37,38]. Since B cells are the critical autoantibody-producing cell type, the B cell numbers were also measured by CD20 staining. The CD20$^+$ B cells were markedly increased in the synovial tissues of Tip60 inhibitor-treated chimeric mice, suggesting that the inhibition of Tip60 acetyltransferase activity can increase the ability of T helper cells to activate B cells. Moreover, the protein expression level of the osteoclastogenic ligand RANKL increased multifold in the synovial tissue (Fig. 6C–E).

To examine the possible link between tissue infiltration, the pro-inflammatory effect and T cell differentiation, we quantified Treg and Th17 subsets using dual-color immunofluorescence staining (Fig. 6F–H). After Tip60 inhibitor treatment, the RA T cells exhibited diffused synovial infiltration and promptly induced the CD3$^+$IL-17$^+$ profile in tissue-infiltrating cells, while the loss of Tip60 function resulted in a significant reduction in Foxp3$^+$ cells (Fig. 6F–H). Immunohistological staining indicated that the downregulation of Foxp3 expression associated with reduced level of acetylated-Foxp3 in the synovial sections from Tip60 inhibitor treated mice than that from control (Fig. 6I and J). Additionally, there are Th17 enrichment and Tregs reduction which were confirmed by the upregulation of the

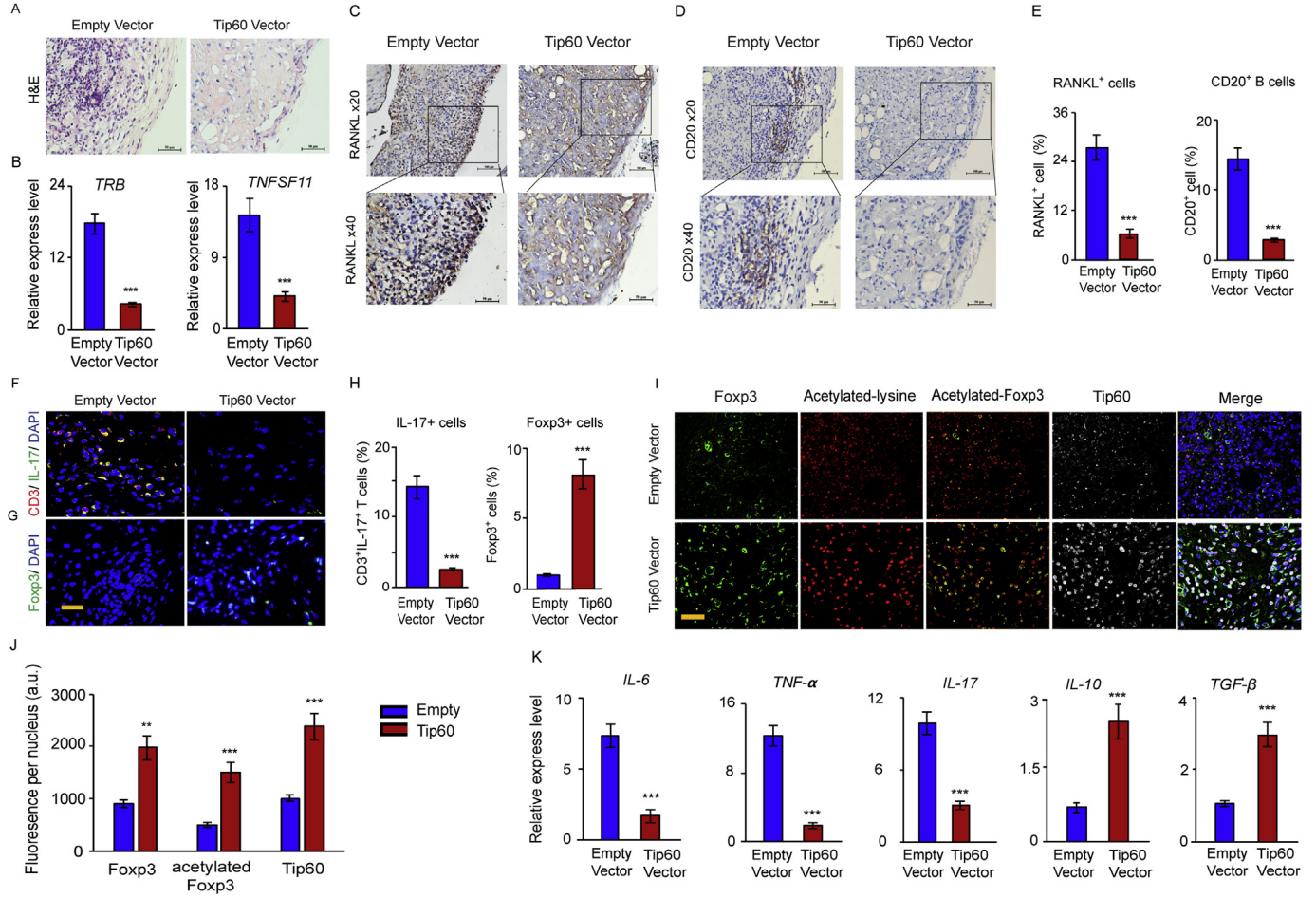

Fig. 7. Restoring Tip60 expression in RA T cells prevents arthritogenic effect. Pairs of NSG mice were engrafted with synovial tissue from RA patients and divided into two treatment groups. $CD45RO^-$ PBMCs from RA patients were transfected with either a control plasmid (pcDNA3.1) or pcDNA3.1-Tip60 and adoptively transferred to the chimeric mice. (A) H&E staining to compare the overall morphology of the synovium from control and Tip60 plasmids transferred chimeric mice. Representative images of the synovium in the control (n = 6) and Tip60 plasmids (n = 6) samples are shown. Bar, 20 μm. (B) The intensity of synovial inflammation was compared by QPCR to assess *TRB* and *TNFSF11* gene expression. The data are representative of three independent experiments. All data are presented as the mean ± SEM from at least 6 different synovial grafts. (C–E) CD20 (C) and RANKL (D) were stained by immunohistochemistry in synovial tissue sections from control and Tip60 plasmid-transfected chimeric mice. The percentages of $CD20^+$ B cells and RANKL-positive cells are presented as the mean ± SEM (E). (F–H) T cell infiltration: (F) Representative images of anti-CD3 (red) and IL-17 staining (green) of the control (n = 6) and Tip60 plasmids (n = 6) samples. $CD3^+IL\text{-}17a^+$ cells are indicated with a yellow coloring. Bar, 20 μm. (G) Representative images of anti-Foxp3 staining (green) of the control (n = 6) and Tip60 plasmids (n = 6) samples. Bar, 20 μm. (H) The percentages of $CD3^+IL\text{-}17a^+$ cells and $Foxp3^+$cells in randomly selected fields of synovial tissue sections are presented as the mean ± SEM. (I) Co-immunostaining of Foxp3 (green), acetylated-lysine (red), and Tip60 (white). Representative images are from one of three synovial tissue from control and Tip60 vector transfected mice. Bar, 20 μm. (J) Fluorescence intensity of Foxp3, acetylated-Foxp3 (combined green and red) and Tip60 are presented as the mean ± SEM. (K) Expression of *IL-6*, *TNF-α*, *IL-17*, *IL-10* and *TGF-β* in the synovium was measured by QPCR. The data are representative of three independent experiments. $^{**}P < 0.01$; $^{***}P < 0.001$. (For interpretation of the references to color in this figure legend, the reader is referred to the Web version of this article.)

proinflammatory cytokines *IL-17, TNF-α* and *IL-6* and the downregulation of the inhibitory cytokines *IL-10* and *TGF-β* (Fig. 6K). These data strongly suggested that the insufficiency of Tip60 acetyltransferase activity increases the proinflammatory effect of T cells by destroying the balance of Treg/Th17 differentiation.

3.7. Restoring Tip60 expression rescues Foxp3 and prevents synovial inflammation

To further understand whether repairing *Tip60* expression in RA $CD4^+$ T cells is sufficient to correct their pathogenic effects, the *Tip60* gene was overexpressed in $CD4^+$ T cells from RA patients prior to adoptive transfer. Ectopic *Tip60* expression strongly attenuated inflammation and immune cell infiltration of the engrafted synovial tissue (Fig. 7A). Specifically, reconstitution of *Tip60* in RA T cells diminished the T cell density, as indicated by decreased *TRB* and *TNFSF11* gene expression (Fig. 7B). Moreover, ectopic expression of *Tip60* acted strongly against inflammation. Transfer of $Tip60^{high}$ RA T cells resulted in downregulation of the B cell number and reduction of RANKL protein expression (Fig. 7C–E). Mechanistic studies indicated that Tip60 protein reconstitution in the transferred T cells corrected dysfunction in T cell lineage commitment, especially decreasing the number of Th17 ($CD3^+IL\text{-}17^+$) cells and increasing the number of $Foxp3^+$ cells in the synovial tissue (Fig. 7F–H). Further staining of synovial sections indicated that Foxp3 expression were upregulated following the rescue of Tip60 and Foxp3 acetylation, indicating that Tip60-regulated Foxp3 acetylation is essential for the $Foxp3^+$ Tregs production in RA patients (Fig. 7I and J). As a result of recovering the Treg/Th17 differentiation balance, the transcript levels of the inflammatory cytokines *TNF-α, IL-6* and *IL-17* were minimized and the levels of the anti-inflammatory cytokines *IL-10* and *TGF-β* were strongly elevated in the synovial tissue (Fig. 7K). These experiments confirmed that Tip60 plays a critical role

in cell infiltration and disease-associated effects of T cells in RA patients, and that restoring Tip60 protein concentrations is sufficient to correct the arthritogenic capability of $CD4^+$ T cells, suggesting Tip60 as a potential therapeutic target for suppression of tissue inflammation and autoimmunity in RA.

4. Discussion

RA patients experience a shift in T cell lineage commitment with a bias toward Th1/Th17 helper cells rather than Tregs, which is the key T cell population that suppresses inflammation and autoimmune responses [2,12]. Here, we demonstrated that the dysfunctional differentiation of naïve T cells in RA patients is critically induced by insufficient expression of the histone acetyltransferase Tip60. Tip60 downregulation not only directly controls Treg/Th17 cell differentiation, but also promotes the production of the proinflammatory cytokines IL-17, TNF-α, and IL-6. The underlying mechanism can be attributed to the reduced Tip60-Foxp3 interaction in T cells of RA patients after stimulation, which leads to the deficiency of Foxp3 acetylation and subsequently Foxp3 degradation. Knockdown or pharmacological inhibition of Tip60 acetyltransferase activity in T cells from healthy donors diminished Foxp3 acetylation, blocked Treg differentiation and re-established the abnormalities present in synovial inflammation. In contrast, overexpression of Tip60 restored Foxp3 expression, normalized T cell differentiation in RA T cells and reversed the severe inflamed phenotype of the RA synovium. Therefore, the Tip60-Foxp3 axis is critical for immunosuppression of T cell function and renders the host more resistant to autoimmune pathogenesis and the development of RA disease.

Tregs are immunosuppressive and thus essential for maintaining the tolerance to self-antigens by suppressing effector T cells. Foxp3 is the crucial transcription factor for Treg development and their inhibitory function. Activated naïve T cells can upregulate the Foxp3 levels. High and stable expression of Foxp3 is essential for Treg maintenance and differentiation after stimulation [39,40]. Acetylation modifications of Foxp3 protein enhance its stability and promote its binding activity [41,42]. In particular, the Tip60 acetylation ligase acts as a critical coactivator of Foxp3, controlling Treg differentiation by increasing the amount of acetylated Foxp3 through protecting Foxp3 from proteasomal degradation. Our study also revealed that activation of naïve T cells triggers the upregulation of Tip60 and a subsequent increase the level of Foxp3 acetylation as well as its concentration, thus promoting Tregs differentiation. Moreover, our data revealed for the first time that naïve $CD4^+$ T cells in RA patients failed to upregulate Tip60 upon stimulation, which directly reduced Foxp3 acetylation and stability, and Tregs production was consequently suppressed.

The Th17 and Treg cell subsets, which are reciprocally interconnected, are major participants in autoimmunity [43,44]. Recent studies indicated that, other than promoting Treg production, the Tip60-Foxp3 components can also physically binds to the Th17-specific transcription factor RORγt and suppress Th17 differentiation by directly suppressing RORγt transcriptional activity [45,46]. Our results confirmed that Tip60 insufficiency was concomitant with a significant increase in the pathogenic Th17 response in RA T cells, suggesting the critical role of Tip60 in keeping the reciprocal differentiation balance of Th17 and Tregs in RA.

The question was raised concerning how the acetyltransferase activity of Tip60 was related to T cell control of synovial inflammation onset *in vivo*. A humanized chimeric mouse model of the human-synovium-NSG mice and human T cells enabled us to investigate the role of Tip60 activity in T cell differentiation and the development of synovial tissue inflammation *in vivo* [47]. We found that inhibition of Tip60 acetyltransferase activity increased the T cells tissue infiltration, suppressed Foxp3 expression, increased the number of Th17 cells, and decreased the number of Tregs, thereby improving the arthritogenic potential of T cells in the synovial microenvironment. In contrast, rescuing Tip60 expression in naïve T cells can effectively attenuate the inflammatory immune response in the synovial tissue by correcting T cell lineage maldifferentiation. Moreover, Tip60 expression was also negatively correlated with B cell number and the RANKL level in the grafted synovial tissue, indicating that Tip60-mediated T cell lineage commitment is critical for inhibiting the inflammatory activity of immune cells and probably tissue-residing cells and maintaining an anti-inflammatory environment in the synovial tissue. These results confirm the importance of Tip60-mediated Treg/Th17 differentiation in autoimmunogenesis in RA.

5. Conclusion

In summary, our experiments demonstrate the critical role of the Tip60-mediated Foxp3 acetylation in attenuated RA progression. Tip60 deficiency in the naïve T cells of RA patients blocks Foxp3 acetylation, downregulates Foxp3 expression, biases the differentiation program toward tissue-infiltration and arthritogenic Th17 cells instead of Tregs. Replenishing Tip60 protein expression by forced overexpression promptly reversed the Treg/Th17 balance of RA T cells. Considering the importance of the Treg/Th17 axis in the pathogenesis of RA, restoring Tip60 represents a new strategy for preventing autoimmunity and blocking inflammatory pathways in RA.

Acknowledgments

We thank all patients and medical staff who generously contributed to this study. All authors have read and approved the final submitted version of the manuscript.

Appendix A. Supplementary data

Supplementary data to this article can be found online at https://doi.org/10.1016/j.jaut.2019.02.007.

Funding

This work was supported by the National Natural Science Foundation of China (grant no. 81671612), the Guangdong Natural Science Foundation (grant no. 2017A030313859 and 2017A030313576), Science and Technology Program of Guangzhou (grant no. 201707010120), and the Fundamental Research Funds for the Central Universities (grant no. 17ykjc 08 and 17ykjc12).

Disclosure statement

The authors declare that they have no competing interests to disclose.

References

[1] I.B. McInnes, G. Schett, The pathogenesis of rheumatoid arthritis, N. Engl. J. Med. 365 (2011) 2205–2219 https://doi.org/10.1056/NEJMra1004965.
[2] J.J. Goronzy, C.M. Weyand, Successful and maladaptive T cell aging, Immunity 46 (2017) 364–378 https://doi.org/10.1016/j.immuni.2017.03.010.
[3] J.J. Goronzy, L. Shao, C.M. Weyand, Immune aging and rheumatoid arthritis, Rheum. Dis. Clin. N. Am. 36 (2010) 297–310 https://doi.org/10.1016/j.rdc.2010.03.001.
[4] E. Boren, M.E. Gershwin, Inflamm-aging: autoimmunity, and the immune-risk phenotype, Autoimmun. Rev. 3 (2004) 401–406 https://doi.org/10.1016/j.autrev.2004.03.004.
[5] L. Shao, H. Fujii, I. Colmegna, H. Oishi, J.J. Goronzy, C.M. Weyand, Deficiency of the DNA repair enzyme ATM in rheumatoid arthritis, J. Exp. Med. 206 (2009) 1435–1449 https://doi.org/10.1084/jem.20082251.
[6] L. Shao, J.J. Goronzy, C.M. Weyand, DNA-dependent protein kinase catalytic subunit mediates T-cell loss in rheumatoid arthritis, EMBO Mol. Med. 2 (2010) 415–427 https://doi.org/10.1002/emmm.201000096.
[7] C.M. Weyand, M. Zeisbrich, J.J. Goronzy, Metabolic signatures of T-cells and macrophages in rheumatoid arthritis, Curr. Opin. Immunol. 46 (2017) 112–120 https://doi.org/10.1016/j.coi.2017.04.010.

[8] C.M. Weyand, J.J. Goronzy, Immunometabolism in early and late stages of rheumatoid arthritis, Nat. Rev. Rheumatol. 13 (2017) 291–301 https://doi.org/10.1038/nrrheum.2017.49.
[9] H. Fujii, L. Shao, I. Colmegna, J.J. Goronzy, C.M. Weyand, Telomerase insufficiency in rheumatoid arthritis, Proc. Natl. Acad. Sci. U. S. A. 106 (2009) 4360–4365 https://doi.org/10.1073/pnas.0811332106.
[10] Z. Yang, H. Fujii, S.V. Mohan, J.J. Goronzy, C.M. Weyand, Phosphofructokinase deficiency impairs ATP generation, autophagy, and redox balance in rheumatoid arthritis T cells, J. Exp. Med. 210 (2013) 2119–2134 https://doi.org/10.1084/jem.20130252.
[11] E. Bettelli, M. Oukka, V.K. Kuchroo, T(H)-17 cells in the circle of immunity and autoimmunity, Nat. Immunol. 8 (2007) 345–350 https://doi.org/10.1038/ni0407-345.
[12] S. Sarkar, D.A. Fox, Targeting IL-17 and Th17 cells in rheumatoid arthritis, Rheum. Dis. Clin. N. Am. 36 (2010) 345–366 https://doi.org/10.1016/j.rdc.2010.02.006.
[13] J.D. Fontenot, M.A. Gavin, A.Y. Rudensky, Foxp3 programs the development and function of CD4+CD25+ regulatory T cells, Nat. Immunol. 4 (2003) 330–336 https://doi.org/10.1038/ni904.
[14] H. Katoh, P. Zheng, Y. Liu, FOXP3: genetic and epigenetic implications for autoimmunity, J. Autoimmun. 41 (2013) 72–78 https://doi.org/10.1016/j.jaut.2012.12.004.
[15] L.M. Williams, A.Y. Rudensky, Maintenance of the Foxp3-dependent developmental program in mature regulatory T cells requires continued expression of Foxp3, Nat. Immunol. 8 (2007) 277–284 https://doi.org/10.1038/ni1437.
[16] Y.Y. Wan, R.A. Flavell, Yin-Yang' functions of transforming growth factor-beta and T regulatory cells in immune regulation, Immunol. Rev. 220 (2007) 199–213 https://doi.org/10.1111/j.1600-065X.2007.00565.x.
[17] X. Du, H. Shi, J. Li, Y. Dong, J. Liang, J. Ye, et al., Mst1/Mst2 regulate development and function of regulatory T cells through modulation of Foxo1/Foxo3 stability in autoimmune disease, J. Immunol. 192 (2014) 1525–1535 https://doi.org/10.4049/jimmunol.1301060.
[18] J. Kamine, B. Elangovan, T. Subramanian, D. Coleman, G. Chinnadurai, Identification of a cellular protein that specifically interacts with the essential cysteine region of the HIV-1 Tat transactivator, Virology 216 (1996) 357–366 https://doi.org/10.1006/viro.1996.0071.
[19] J.H. Kim, B. Kim, L. Cai, H.J. Choi, K.A. Ohgi, C. Tran, et al., Transcriptional regulation of a metastasis suppressor gene by Tip60 and beta-catenin complexes, Nature 434 (2005) 921–926 https://doi.org/10.1038/nature03452.
[20] V. Sapountzi, I.R. Logan, C.N. Robson, Cellular functions of TIP60, Int. J. Biochem. Cell Biol. 38 (2006) 1496–1509 https://doi.org/10.1016/j.biocel.2006.03.003.
[21] T. Ikura, V.V. Ogryzko, M. Grigoriev, R. Groisman, J. Wang, M. Horikoshi, et al., Involvement of the TIP60 histone acetylase complex in DNA repair and apoptosis, Cell 102 (2000) 463–473 https://www.ncbi.nlm.nih.gov/pubmed/10966108.
[22] G. Yang, B.H. Cheng, S.B. Yang, Z.Q. Liu, S.Q. Qiu, L.T. Yang, et al., Targeting histone-acetyltransferase Tat-interactive protein 60 inhibits intestinal allergy, Allergy 73 (2018) 387–394 https://doi.org/10.1111/all.13304.
[23] F. Mo, X. Zhuang, X. Liu, P.Y. Yao, B. Qin, Z. Su, et al., Acetylation of Aurora B by TIP60 ensures accurate chromosomal segregation, Nat. Chem. Biol. 12 (2016) 226–232 https://doi.org/10.1038/nchembio.2017.
[24] Y. Sun, X. Jiang, B.D. Price, Tip60: connecting chromatin to DNA damage signaling, Cell Cycle 9 (2010) 930–936 https://doi.org/10.4161/cc.9.5.10931.
[25] C.H. Kim, J.W. Kim, S.M. Jang, J.H. An, S.B. Seo, K.H. Choi, The chromodomain-containing histone acetyltransferase TIP60 acts as a code reader, recognizing the epigenetic codes for initiating transcription, Biosci. Biotechnol. Biochem. 79 (2015) 532–538 https://doi.org/10.1080/09168451.2014.993914.
[26] M. Ikura, K. Furuya, S. Matsuda, R. Matsuda, H. Shima, J. Adachi, et al., Acetylation of histone H2AX at lys 5 by the TIP60 histone acetyltransferase complex is essential for the dynamic binding of NBS1 to damaged chromatin, Mol. Cell Biol. 35 (2015) 4147–4157 https://doi.org/10.1128/MCB.00757-15.
[27] J. van Loosdregt, P.J. Coffer, Post-translational modification networks regulating FOXP3 function, Trends Immunol. 35 (2014) 368–378 https://doi.org/10.1016/j.it.2014.06.005.
[28] J. Li, X. Du, H. Shi, K. Deng, H. Chi, W. Tao, Mammalian sterile 20-like kinase 1 (Mst1) enhances the stability of forkhead box P3 (Foxp3) and the function of regulatory T cells by modulating Foxp3 acetylation, J. Biol. Chem. 290 (2015) 30762–30770 https://doi.org/10.1074/jbc.M115.668442.
[29] M.L. Bettini, F. Pan, M. Bettini, D. Finkelstein, J.E. Rehg, S. Floess, et al., Loss of epigenetic modification driven by the Foxp3 transcription factor leads to regulatory T cell insufficiency, Immunity 36 (2012) 717–730 https://doi.org/10.1016/j.immuni.2012.03.020.
[30] J. Geng, S. Yu, H. Zhao, X. Sun, X. Li, P. Wang, et al., The transcriptional coactivator TAZ regulates reciprocal differentiation of TH17 cells and Treg cells, Nat. Immunol. 18 (2017) 800–812 https://doi.org/10.1038/ni.3748.
[31] J. Xiao, C. Liu, G. Li, S. Peng, J. Hu, L. Qu, et al., PDCD5 negatively regulates autoimmunity by upregulating FOXP3(+) regulatory T cells and suppressing Th17 and Th1 responses, J. Autoimmun. 47 (2013) 34–44 https://doi.org/10.1016/j.jaut.2013.08.002.
[32] F.C. Arnett, S.M. Edworthy, D.A. Bloch, D.J. McShane, J.F. Fries, N.S. Cooper, et al., The American Rheumatism Association 1987 revised criteria for the classification of rheumatoid arthritis, Arthritis Rheum. 31 (1988) 315–324 https://www.ncbi.nlm.nih.gov/pubmed/3358796.
[33] L. Shao, H.J. Zhou, H. Zhang, L. Qin, J. Hwa, Z. Yun, et al., SENP1-mediated NEMO deSUMOylation in adipocytes limits inflammatory responses and type-1 diabetes progression, Nat. Commun. 6 (2015) 8917 https://doi.org/10.1038/ncomms9917.
[34] T.M. Seyler, Y.W. Park, S. Takemura, R.J. Bram, P.J. Kurtin, J.J. Goronzy, et al., BLyS and APRIL in rheumatoid arthritis, J. Clin. Investig. 115 (2005) 3083–3092 https://doi.org/10.1172/JCI25265.
[35] Y. Li, Y. Shen, P. Hohensinner, J. Ju, Z. Wen, S.B. Goodman, et al., Deficient activity of the nuclease MRE11A induces T cell aging and promotes arthritogenic effector functions in patients with rheumatoid arthritis, Immunity 45 (2016) 903–916 https://doi.org/10.1016/j.immuni.2016.09.013.
[36] J.D. Ma, J.J. Zhou, D.H. Zheng, L.F. Chen, Y.Q. Mo, X.N. Wei, et al., Serum matrix metalloproteinase-3 as a noninvasive biomarker of histological synovitis for diagnosis of rheumatoid arthritis, Mediat. Inflamm. 2014 (2014) 179284 https://doi.org/10.1155/2014/179284.
[37] G. Schett, S. Hayer, J. Zwerina, K. Redlich, J.S. Smolen, Mechanisms of Disease: the link between RANKL and arthritic bone disease, Nat. Clin. Pract. Rheumatol. 1 (2005) 47–54 https://doi.org/10.1038/ncprheum0036.
[38] R. Schlegel, A.B. Pardee, Caffeine-induced uncoupling of mitosis from the completion of DNA replication in mammalian cells, Science 232 (1986) 1264–1266 https://www.ncbi.nlm.nih.gov/pubmed/2422760.
[39] M.A. Gavin, T.R. Torgerson, E. Houston, P. DeRoos, W.Y. Ho, A. Stray-Pedersen, et al., Single-cell analysis of normal and FOXP3-mutant human T cells: FOXP3 expression without regulatory T cell development, Proc. Natl. Acad. Sci. U. S. A. 103 (2006) 6659–6664 https://doi.org/10.1073/pnas.0509484103.
[40] S.E. Allan, A.N. Alstad, N. Merindol, N.K. Crellin, M. Amendola, R. Bacchetta, et al., Generation of potent and stable human CD4+ T regulatory cells by activation-independent expression of FOXP3, Mol. Ther. 16 (2008) 194–202 https://doi.org/10.1038/sj.mt.6300341.
[41] B. Li, M.I. Greene, FOXP3 actively represses transcription by recruiting the HAT/HDAC complex, Cell Cycle 6 (2007) 1432–1436 https://www.ncbi.nlm.nih.gov/pubmed/17592252.
[42] U.H. Beier, T. Akimova, Y. Liu, L. Wang, W.W. Hancock, Histone/protein deacetylases control Foxp3 expression and the heat shock response of T-regulatory cells, Curr. Opin. Immunol. 23 (2011) 670–678 https://doi.org/10.1016/j.coi.2011.07.002.
[43] T. Korn, E. Bettelli, M. Oukka, V.K. Kuchroo, IL-17 and Th17 cells, Annu. Rev. Immunol. 27 (2009) 485–517 https://doi.org/10.1146/annurev.immunol.021908.132710.
[44] D.R. Littman, A.Y. Rudensky, Th17 and regulatory T cells in mediating and restraining inflammation, Cell 140 (2010) 845–858 https://doi.org/10.1016/j.cell.2010.02.021.
[45] X.O. Yang, R. Nurieva, G.J. Martinez, H.S. Kang, Y. Chung, B.P. Pappu, et al., Molecular antagonism and plasticity of regulatory and inflammatory T cell programs, Immunity 29 (2008) 44–56 https://doi.org/10.1016/j.immuni.2008.05.007.
[46] L. Zhou, M.M. Chong, D.R. Littman, Plasticity of CD4+ T cell lineage differentiation, Immunity 30 (2009) 646–655 https://doi.org/10.1016/j.immuni.2009.05.001.
[47] S.H. Hwang, S.H. Jung, S. Lee, S. Choi, S.A. Yoo, J.H. Park, et al., Leukocyte-specific protein 1 regulates T-cell migration in rheumatoid arthritis, Proc. Natl. Acad. Sci. U. S. A. 112 (2015) E6535–E6543 https://doi.org/10.1073/pnas.1514152112.